JOURNAL OF AGRICULTURAL AND FOOD CHEMISTRY

Validation of Antifreeze Properties of Glutathione Based on Its Thermodynamic Characteristics and Protection of Baker's Yeast during Cryopreservation

CHAO ZHANG,[†,‡] HUI ZHANG,*[,†,‡] LI WANG,[†] AND HUIYUAN YAO[†]

Key Laboratory of Food Science and Technology and School of Food Science and Technology, Southern Yangtze University, 1800 Lihu Avenue, Wuxi 214122, China

The antifreeze ability of glutathione was evaluated on the basis of its thermodynamic characteristics and protection of baker's yeast during cryopreservation at −30 °C. The thermodynamic characteristics and protection of baker's yeast of glutathione were similar to those of known antifreeze proteins, such as carrot antifreeze protein and holly antifreeze protein. These properties included lowering the freezing point at about 0.20 °C non-colligatively, decreasing freezable water content, controlling the movement of free water for its strong hydrophilicity, and improving baker's yeast survival during the simulated processing of frozen dough. Therefore, glutathione was viewed to be an antifreeze protein like substance on the basis of its unique thermodynamic characteristics and protection of baker's yeast. The method combining thermodynamic characteristic analysis and protection evaluation is a new and simple way to screen new antifreeze proteins.

KEYWORDS: Antifreeze protein; glutathione; thermodynamic characteristic; cryopreservation; baker's yeast

INTRODUCTION

Glutathione (GSH), which is found in all mammalian cells, plays an important chemical and metabolic function in general and protective ability during cryopreservation in particular (*1*). For example, adding GSH to preservation solution improves the survival of the liver cell during cryopreservation (*2*). GSH can also protect membranes of sperms or oocytes from lipid peroxidation by scavenging reactive oxygen species during cryopreservation (*3*, *4*). Moreover, the viability and motility of spermatozoa can be improved by adding GSH during cryopreservation, because GSH prevents peroxidative damage to cell membranes, DNA, and proteins (*5*−*7*). In all of these studies, GSH played the factual role of an antifreeze protein (AFP).

AFP was first found in fish; it lowered the freezing point of fish blood below the freezing point of seawater to prevent fish from freezing (*8*). All AFPs lower the freezing point non-colligatively and show thermal hysteresis activity (THA), that is, the temperature difference between the non-colligative freezing point and the colligative melting point (*9*). In addition, AFP has a strong hydrophilic ability to control the movement of free water (*10*, *11*). AFP has been applied to food processing, cryopreservation of organs or cells, cryosurgery, and aquaculture (*10*, *12*). Up to now, studies have shown that AFP enhances the survival rate of yeast and viability of sperm from rams, chimpanzees, stallions, and ox during cryopreservation by lowering the freezing point and decreasing the freezable water content (*10*, *13*−*16*).

There is little known of the similarity and dissimilarity between GSH and AFP, although they have in common in the protection of living cells during cryopreservation. Previous studies have paid more attention to the chemical and metabolic functions of GSH in protecting cells during cryopreservation. The physical and thermodynamic characteristics of GSH related to its antifreeze properties have been neglected so far. Therefore, we studied the physical and thermodynamic characteristics of GSH by differential scanning calorimetry (DSC) and thermal gravimetric analysis (TGA) to validate GSH as a potential AFP. We also studied its protection of baker's yeast frozen at −30 °C, the condition of frozen dough processing. Furthermore, the method used could be a new tool to screen new AFP sources on the basis of their physical and thermodynamic characteristics and protection validation during cryopreservation.

MATERIALS AND METHODS

Assay of GSH Content. Total GSH (Sigma Chemical, Co., St. Louis, MO) content was measured by the GSH assay as modified by Tietze (*17*). Sample was placed in 1 M perchloric acid containing 2 mM EDTA and centrifuged at 3000*g* for 15 min. The supernatant was neutralized with 4 M KOH containing 0.6 M Mops (Sigma Chemical) and then centrifuged at 3000*g* for 15 min. The supernatant was measured with a spectrophotometer (no. 752, Shanghai Spectrum Instrument Co., Shanghai, China) at 412 nm by a GSH reductase-linked 5,5′-dithiobis-(2-nitrobenzoic acid) assay. Quantification was based on standard curves prepared with known GSH concentrations.

* Author to whom correspondence should be addressed (telephone/fax +86-510-85919101; e-mail loszc@hotmail.com).
† Key Laboratory of Food Science and Technology.
‡ School of Food Science and Technology.

10.1021/jf070387q CCC: $37.00
Published on Web 05/18/2007

Preparation of Carrot (*Daucus carota*) AFP. Carrot (*D. carota*) antifreeze protein (*Dc*AFP) was purified and lyophilized following the procedure described by Meyer et al. (*18*). The cold-acclimated carrot taproots were purchased from a local supermarket. The protein content of *Dc*AFP solution was evaluated by Coomassie Brilliant Blue G-250.

Evaluation of Thermodynamic Characteristics and THA by DSC Method. Thermodynamic characteristics and THA were measured by DSC method (Diamond DSC-7, Perkin-Elmer Pyris, Boston, MA). An aliquot of 10 μL of protein solution [including bovine serum albumin (BSA), *Dc*AFP, and GSH, respectively, with a final protein content of 2 mg/mL evaluated by Coomassie Brilliant Blue G-250] was sealed in a preweighed aluminum pan. The sample was cooled from 20 to −30 °C at the rate of 3 °C/min and held for 15 min, followed by heating to 20 °C at the rate of 3 °C/min. The melting point (T_m) and exothermic area (ΔA_m) were calculated by Pyris Software for Windows, version 3.80. Then, the sample was cooled from 20 to −30 °C at the rate of 3 °C/min, held for 15 min, and then heated to the holding temperature (T_h) when the system was at phase equilibrium with the solid (ice crystal) and liquid (aqueous solution). After 2 min of holding at the T_h, the sample was cooled from T_h to −30 °C at the rate of 3 °C/min. The exothermic area (ΔA_f) and onset temperature (T_o) were recorded. This process was repeated at different T_h. Water was used as the control. The ice crystal content (ϕ) and THA were calculated by the formulas below, as described by Chen et al. (*19*):

$$\phi = 1 - \frac{\Delta A_f}{\Delta A_m} \quad (1)$$

where ΔA_f is the exothermic area after holding at T_h and ΔA_m is the exothermic area during the freezing process.

THA is expressed as

$$\mathrm{THA} = T_h - T_o \quad (2)$$

where T_h is the holding temperature and T_o is the onset temperature when the exothermic process begins.

Determination of Freezable Water Content by DSC Method. The freezable water content (Δ) of the protein solution [including BSA, *Dc*AFP, and GSH, respectively, with final protein concentration (W_A) of 10, 20, 30, 40, and 50% (w/v)] was determined by DSC (Diamond DSC-7, Perkin-Elmer Pyris) (*20*). The freezable water content in sample (W_C) was determined by DSC with the following process. An aliquot of 10 μL of sample was sealed in an aluminum pan and stored at −30 °C for 48 h. Then the sealed sample was quickly moved to a prefrozen stove of DSC with an empty aluminum pan as reference, holding at −30 °C for 15 min, and then the temperature was raised to 15 °C at the rate of 3 °C/min. The endothermic enthalpy (ΔH_W) of sample was recorded (statistical analysis done by Pyris Software for Windows, version 3.80). The W_C was counted by endothermic enthalpy of water ($\Delta_{fus}H_m$ = 333.3 J/g).

The freezable water content in protein solution (W_C) is expressed as

$$W_C = \frac{\Delta H_W}{\Delta_{fus}H_m \times m} \quad (3)$$

where ΔH_W is endothermic enthalpy (J) of sample, $\Delta_{fus}H_m$ = 333.3 J/g, and m is sample weight (g).

The freezable water content (Δ) is expressed as

$$\Delta = \frac{W_C}{W_A} \times 100\% \quad (4)$$

where W_C is the freezable water content of sample and W_A is the moisture content of sample.

Hydrophilic Ability Evaluated by Thermal Gravimetric Analysis (TGA) Method. The thermal gravimetric analyzer was heated from 30 to 800 °C at a rate of 15 °C/min with a nitrogen flow of 40 mL/min by TGA/SDTA 851^e (Mettler-Toledo GmbH, Schwerzenbach, Switzerland) (*21*, *22*). Aliquots of 20 μL of sample [including BSA, *Dc*AFP, and GSH, respectively, with a final protein content at 10% (w/v)] were loaded into 70 μL ceramic pans. Water was used as the control. The TGA curve showed weight loss during the heating process. A synchronal different temperature analysis (SDTA) curve displayed the temperature difference between the cell and the sample.

Evaluation of Baker's Yeast (*Saccharomyces cerevisiae*) Survival Rate during Cryopreservation by Plate-Counting Method. An aliquot of 500 mg of baker's yeast (*S. cerevisiae*, CBS 8066, Baarn, The Netherlands) was suspended in 1 L of 0.9% (w/v) physiological saline solution. Protein, including BSA, *Dc*AFP, and GSH, respectively, was added to the yeast suspension, resulting in a final protein concentration of 10% (w/v). The control had the same formula except protein. Aliquots of 3 mL of the above suspension were transferred to test tubes and stored at −30 °C for 1−10 weeks. After cryopreservation at −30 °C, the suspension was thawed at 25 °C for about 20 min, and the survival of the yeast was determined by plate counting. Each batch was counted three times. After incubation at 30 °C for 48 h, the number of grown colonies was determined and the survival of yeast was calculated as the ratio of the number of colonies grown after cryopreservation to the number of colonies grown without cryopreservation (*23*).

Statistical Analysis. Data were expressed as the mean value ± standard deviation (n = 3). All statistical analyses were done with the Super ANOVA (version 1.11, Abacus Concepts Inc., Berkeley, CA). One-way ANOVA and multiple comparisons (Fisher's least significant difference test) were used to evaluate the significant differences of the data at the criterion of $P < 0.05$.

RESULTS AND DISCUSSION

Thermodynamic Characteristics and THA of GSH. Figure 1 shows the freeze−thaw thermograph of the control, BSA, and *Dc*AFP solutions. Only one peak presented in the endothermic and exothermic process, respectively, in the thermograph of the control, BSA, or *Dc*AFP solution. The thermograph peaks of the three tested solutions were smooth in the endothermic process and steep in the exothermic process. In contrast, **Figure 2** shows the freeze−thaw thermograph of the GSH solution. The thermograph of the GSH solution had two exothermic peaks and two endothermic peaks during the freeze−thaw process, respectively, different from those of the control, BSA, and *Dc*AFP solutions. The double peak indicated that the thermodynamic characteristic of the GSH solution was more complicated than those of other three tested solutions. Meanwhile, the thermograph of the GSH solution was smooth in the endothermic process and steep in the exothermic process, similar to those of the other three tested solutions. Our study described for the first time that the double peak of GSH appeared during the freeze−thaw process. Double-peak appearance in the freeze−thaw process was reported from only holly (*Ammopiptanthus mongolicus*) protein solution, a known AFP found by Chen et al. (*19*). Meanwhile, Chen pointed out that the double-peak presents only in certain AFPs (*19*). In our study, we found the double-peak appearance in GSH, which implied similarity in thermodynamic characteristics of GSH to those of holly AFP. Therefore, the GSH had certain similar thermodynamic characteristics to an AFP. On the other hand, the THA was not shown in **Figures 1** and **2**, because of the supercooling of the tested solutions. Therefore, the freezing points were −17.75, −22.26, −16.84, and −21.84 °C in the thermograph of the control, BSA, *Dc*AFP, and GSH solutions, respectively, much lower than the normal freezing point, such as that for water at 0 °C or that for fish at −2.6 °C (*8*).

The areas of peaks 1 and 2 were different in both the exothermic and endothermic processes, respectively, as shown in **Figure 2**. The area of peak 1 was 1081 mJ in the endothermic process and 63.24% of the exothermic area (−1711 mJ). The area of peak 2 was 426.0 mJ in the endothermic process and 97.12% of the exothermic area (−438.6 mJ). Peaks 1 and 2

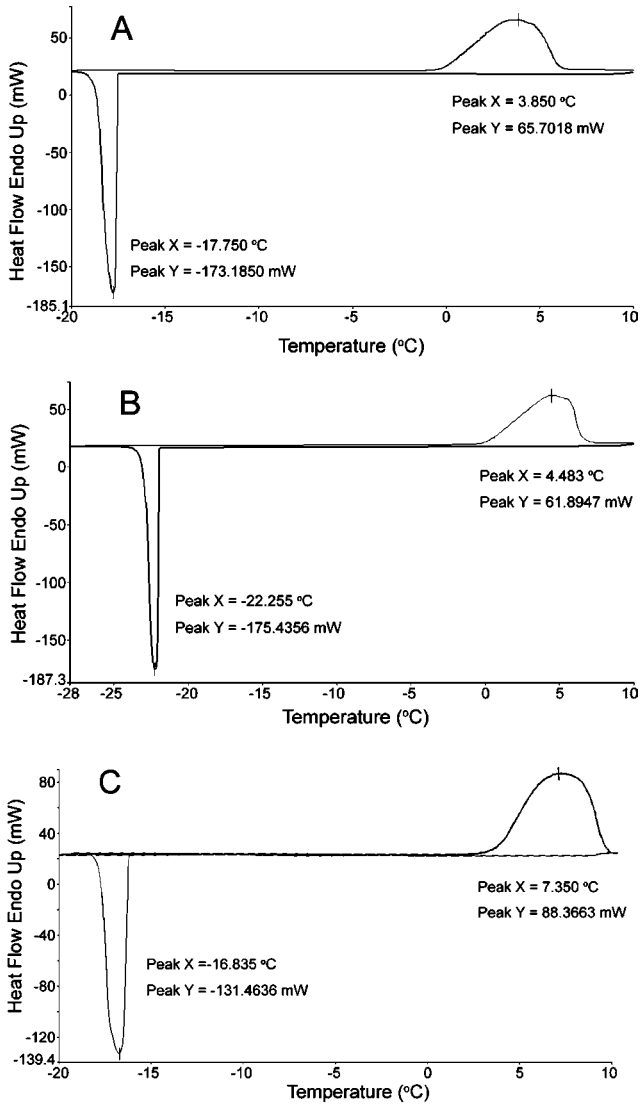

Figure 1. Freeze–thaw thermograph of the control (**A**), BSA (**B**), and *Dc*AFP (**C**) solutions. The freeze–thaw thermograph of the sample is measured by DSC at a rate of 3 °C/min.

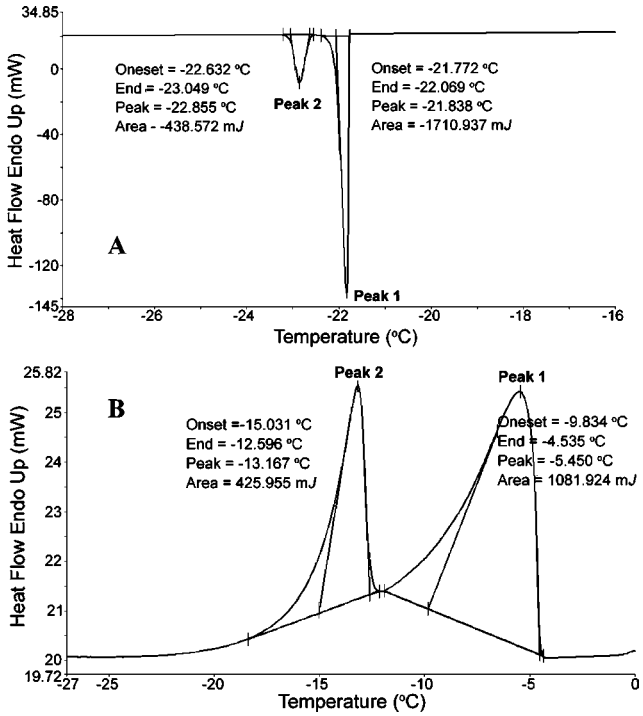

Figure 2. Freeze–thaw thermograph of the GSH solution: (**A**) freezing thermograph; (**B**) thawing thermograph. The endothermic area and exothermic area of the sample are measured by DSC.

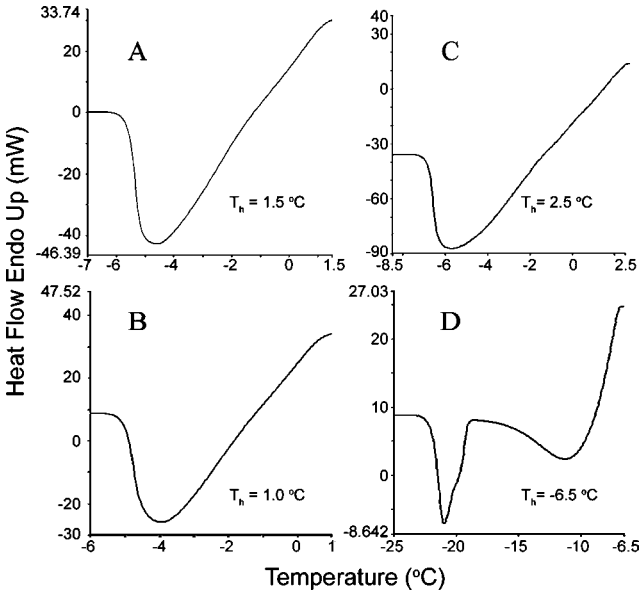

Figure 3. Determination of thermal hysteresis activity of the control (**A**, $T_h = 1.5$ °C), BSA (**B**, $T_h = 1.0$ °C), *Dc*AFP (**C**, $T_h = 2.5$ °C), and GSH solutions (**D**, $T_h = -6.5$ °C) by DSC. The thermographs indicate the exothermic process and thermal hysteresis activity when the sample is frozen after holding at its corresponding T_h for 2.0 min.

were overlapped in the endothermic process. In contrast, peaks 1 and 2 were separated in the exothermic process. Therefore, the area was accurate in the exothermic process and the sum area (ΔA_m) was −2149 mJ.

Figure 3 shows the exothermic thermograph of the control, BSA, *Dc*AFP, and GSH solutions after holding at their corresponding T_h for 2 min. The thermograph of the control, BSA, and *Dc*AFP solutions had only one smooth exothermic peak at −4.62, −5.73, and −5.92 °C, respectively. In contrast, the thermograph of GSH had peak 1 at −11.53 °C and peak 2 at −21.05 °C. Meanwhile, the double peak of the GSH solution presented in all holding temperatures, similar to that of holly AFP and different from those of the control and BSA solutions. These exothermic peaks were much lower than those shown in **Figures 1** and **2** and reinforced the supercooling state described above. These results proved that the used DSC method measured THA accurately and prevented the supercooling state effectively. Furthermore, the thermograph of *Dc*AFP was a typical curve of AFPs (*24*) and showed that the THA of *Dc*AFP was 0.22 °C when the T_h was 2.5 °C. In our study, the THA of GSH was 0.17 °C when the T_h was −6.5 °C, similar to that of *Dc*AFP. In contrast, the control and BSA solutions did not show THA at any T_h. Therefore, the thermodynamic characteristic of GSH was different from those of the control and BSA and was similar to that of *Dc*AFP, concerning the THA. This confirmed that the thermodynamic characteristic of GSH was similar to that of *Dc*AFP or other known AFPs.

Figure 4 shows the effect of ice crystal content (ϕ) on THA of *Dc*AFP and GSH. The THA of *Dc*AFP and GSH decreased when ϕ increased. Similar trends have been proven in fish AFP and insect AFP (*25*, *26*). Furthermore, the THA of GSH was

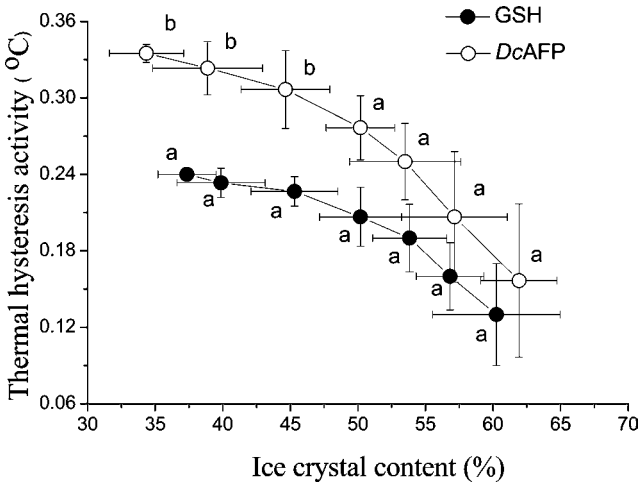

Figure 4. Effect of ice crystal content (ϕ, %) on thermal hysteresis activity of *Dc*AFP and GSH. Ice crystal content and thermal hysteresis activity are measured by DSC. Data are means ± standard deviation ($n = 3$). Means with different letters represent a significant difference ($P < 0.05$).

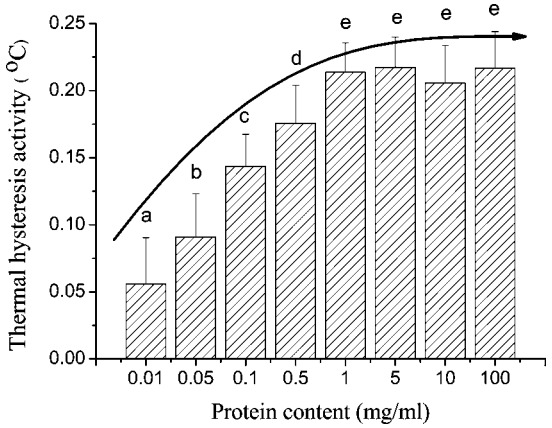

Figure 5. Effect of protein content on the THA of GSH. THA is determined by DSC with ice crystal content at 50 ± 5%. The arrow shows the trends of THA, which holds at about 0.20 °C after the GSH content is >1 mg/mL. Data are means ± standard deviation ($n = 3$). Means with different letters represent a significant difference ($P < 0.05$).

similar to that of *Dc*AFP statistically when ϕ was from 45 to 65%, morer evidence proving GSH with AFP feature.

Figure 5 shows the effect of GSH content on THA when ϕ was at 50 ± 5%. The THA was raised when the GSH content increased from 0.01 to 1 mg/mL, and THA was held at about 0.2 °C when GSH content ranged from 1 to 100 mg/mL. Nevertheless, cryoprotective agents, such as dimethyl sulfoxide, acetamide, glycerol, sucrose, and salt, lower the freezing point colligatively, different from that of AFP (*27*). AFP lowers the freezing point non-colligatively and holds at a certain THA when the protein content exceeds the threshold (*9*). GSH showed similar THA trends as for the AFP, and the threshold of GSH was at about 1 mg/mL.

The double-peak thermograph of GSH was similar to that of holly AFP (*19*, *28*). The THA and THA trend of GSH were similar to those of *Dc*AFP and different from those of the control and BSA solutions. In conclusion, GSH had thermodynamic characteristics and THA similar to those of AFPs including *Dc*AFP and holly AFP. On the other hand, the definition of AFP is rather controversial until now (*25*). However, AFPs have some common properties, such as lowering the freezing point

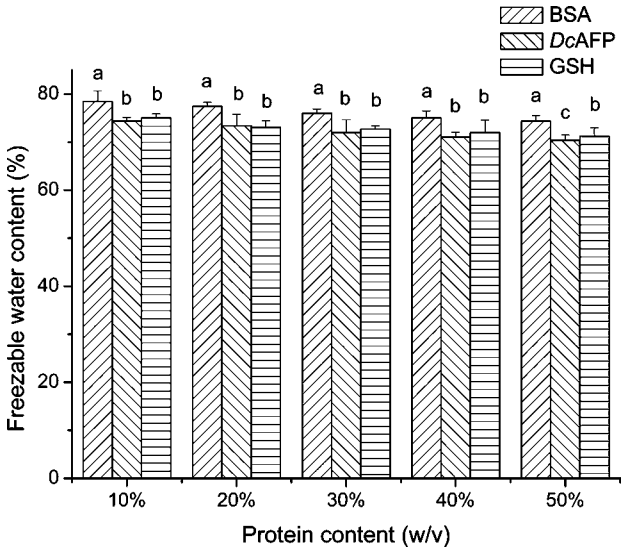

Figure 6. Effect of protein content on freezable water content. Freezable water content is determined by DSC. Data are means ± standard deviation ($n = 3$). Means with different letters represent a significant difference ($P < 0.05$).

non-colligatively, decreasing the osmotic pressure, and inhibiting the recrystallization (*8*, *10*). Remarkably, lowering the freezing point non-colligatively is a unique property of AFP (*8*, *9*). GSH had the ability to lower the freezing point non-colligatively (**Figure 5**). Therefore, GSH was an AFP and had the unique antifreeze property.

Freezable Water Content (Δ) of the GSH Solution Evaluated by DSC Method. Figure 6 shows the effect of protein content on freezable water content. The freezable water content decreased when the protein content increased in BSA, *Dc*AFP, and GSH solutions. The BSA, *Dc*AFP, and GSH solutions showed similar trends of freezable water content. However, statistical analysis indicated that the freezable water content of *Dc*AFP and GSH solutions showed significant differences from that of the BSA solution ($P < 0.05$). The freezable water content of the *Dc*AFP solution was statistically similar to that of the GSH solution when the protein content ranged from 10 to 40% (w/v). Therefore, the GSH solution had characteristics similar to those of the *Dc*AFP solution in regard to the freezable water content.

The freezable water content reflects the content of the free water in the solution and the hydrophilicity of the solute. When the solute has strong hydrophilic ability, the content of the free water is low, and vice versa (*29*). The freezable water content of the *Dc*AFP and GSH solutions was lower than that of the BSA solution. Therefore, the hydrophilic ability of the *Dc*AFP and GSH solution was higher than that of the BSA solution. The *Dc*AFP solution and all AFPs have strong hydrophilic ability to control the movement of free water (*10*, *11*, *25*, *26*). The GSH solution showed a hydrophilic ability statistically similar to that of the *Dc*AFP solution. Therefore, the GSH solution also had strong hydrophilic ability. This confirmed that the strong hydrophilicity of GSH was similar to that of *Dc*AFP or other known AFPs.

Hydrophilic Ability of the Four Tested Solutions Evaluated by TGA Method. Figure 7 shows the TGA and SDTA curves of the control, BSA, *Dc*AFP, and GSH solutions. We monitored the exact temperature at which the sample weight loss was 90%, because the samples of the BSA, *Dc*AFP, and GSH solutions all had 10% (w/v) protein. The temperatures were 148, 168, 178, and 175 °C for the control, BSA, *Dc*AFP, and

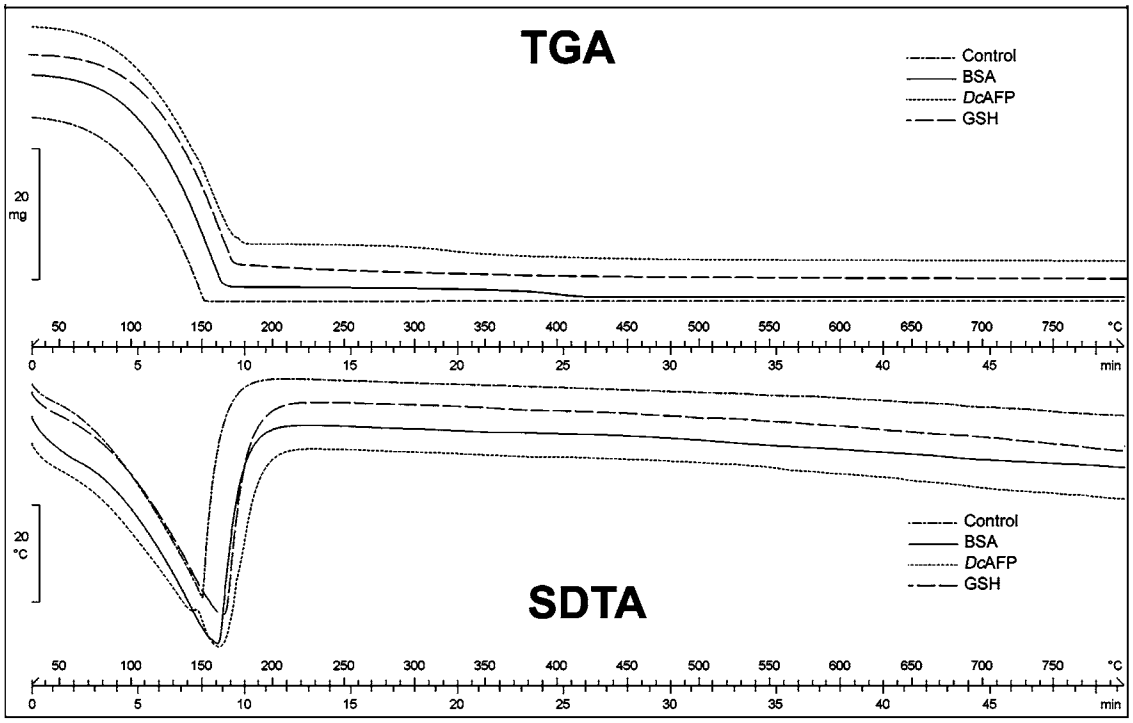

Figure 7. TGA (top) and SDTA (bottom) curves of the control, BSA, *Dc*AFP, and GSH. Sample is heated from 30 to 800 °C at a rate of 15 °C/min with nitrogen flow at 40 mL/min.

GSH solutions, respectively, when the weight loss was 90%. The *Dc*AFP and GSH solution had higher temperature for 90% weight loss than those of the control and BSA solutions. Therefore, the water of *Dc*AFP and GSH cost more time to escape from the protein solution than that of the control and BSA solutions. Meanwhile, the SDTA curves of the four tested solutions showed similar results. The water evaporation of the four tested solutions resulted in big temperature differences between cell and sample in SDTA curves. The water evaporation of the control, BSA, *Dc*AFP, and GSH solutions stopped at about 195, 206, 218, and 220 °C, respectively, as inferred from the SDTA curves.

The water of the *Dc*AFP solution takes more time to evaporate because of the strong hydrophilicity of *Dc*AFP (*10*). Meanwhile, all AFPs have strong hydrophilicity (*25*, *26*). Remarkably, the time required for the GSH solution to evaporate 90% weight was similar to that of the *Dc*AFP solution. In addition, GSH had a strong hydrophilic ability structurally, because it was composed of three hydrophilic amino acids. In conclusion, GSH had a strong hydrophilicity, similar to that of the *Dc*AFP or other known AFPs.

Effect of Cryopreservation at −30 °C on Baker's Yeast (*S. cerevisiae*, CBS 8066) Survival Rate. Table 1 shows the effect of cryopreservation at −30 °C on baker's yeast (*S. cerevisiae*, CBS 8066) survival. The yeast survival rate in the control, BSA, *Dc*AFP, and GSH solutions decreased during the cryopreservation. Moreover, the yeast survival rate in the *Dc*AFP and GSH solutions showed significant difference from that in the control ($P < 0.05$). Meanwhile, statistical analysis showed that the yeast survival rate in the *Dc*AFP and GSH solutions was higher than that in the control and BSA solutions after 1 week of cryopreservation. The yeast survival rate in the GSH solution was statistically similar to that in the *Dc*AFP solution. In our previous study, *Dc*AFP raises the yeast survival rate by lowering the freezing point and decreasing the freezable water content during cryopreservation (*10*). The GSH solution also presented a protective ability to yeast similar to that shown by the *Dc*AFP solution during cryopreservation. Remarkably, the condition of cryopreservation in this experiment was the same as the processing of frozen dough described earlier (*10*). Because of its similarity to *Dc*AFP, GSH could also be potentially used to improve yeast survival in frozen dough. More potential applications are open to GSH as an antifreeze agent.

Table 1. Effect of Cryopreservation at –30 °C on Baker's Yeast Survival Rate[a] (σ)

week	control	BSA	*Dc*AFP	GSH
0	75.15 ± 2.23 a	75.15 ± 2.23 a	75.15 ± 2.23 a	75.15 ± 2.23 a
1	71.20 ± 2.67 a	71.61 ± 1.20 a	74.57 ± 2.30 b	73.12 ± 1.43 b
2	64.44 ± 1.57 a	69.30 ± 2.67 b	74.32 ± 2.45 c	72.35 ± 2.45 c
3	59.94 ± 3.10 a	62.57 ± 2.45 a	73.73 ± 1.45 b	70.65 ± 2.10 b
4	52.00 ± 2.45 a	59.10 ± 0.53 b	72.62 ± 2.67 c	66.70 ± 2.52 b
5	51.00 ± 0.80 a	55.40 ± 1.57 a	68.90 ± 1.57 b	60.04 ± 2.67 b
6	45.14 ± 2.40 a	53.25 ± 2.10 a	67.62 ± 2.10 c	59.63 ± 1.57 b
7	43.86 ± 2.10 a	51.07 ± 2.80 b	63.65 ± 3.10 b	55.77 ± 3.10 b
8	41.23 ± 1.40 a	46.53 ± 0.90 b	62.37 ± 0.70 c	51.20 ± 0.59 b
9	40.80 ± 3.10 a	45.88 ± 3.10 b	61.27 ± 1.13 d	54.93 ± 0.90 c

[a] The survival rate of baker's yeast (*S. cerevisiae*, CBS 8066) is determined by plate-counting. Data are means ± standard deviation ($n = 3$). Data in the same row with different letters are significantly different ($P < 0.05$).

Two main reasons explained why GSH protected baker's yeast similarly to *Dc*AFP during the simulated processing of frozen dough. The first is, as derived from early studies based mainly on the chemical and metabolic functions of GSH, that GSH can improve the cell survival rate by scavenging free radicals or raising viability and raising motility of spermatozoa by preventing peroxidative damage to cell membranes, DNA, and proteins during cryopreservation (*2*−*7*, *30*). The second reason is, due to its physical and thermodynamic characteristics, that GSH lowers the freezing point, decreases the freezable water content, and controls the movement of free water for its hydrophilicity during cryopreservation, playing an important role in the protection of baker' yeast (*10*). Nevertheless, physical and thermodynamic characteristics were shadowed by the strong

chemical and metabolic functions of GSH in previous studies. We presented a comprehensive view describing GSH's protection of baker's yeast during cryopreservation. On the basis of these results, GSH could be probably applied as an AFP in cryopreservation. Moreover, we provide a new tool to screen new AFPs based on the combination of thermodynamic characteristics and protection ability.

ABBREVIATIONS USED

AFP, antifreeze protein; BSA, bovine serum albumin; *Dc*AFP, *Daucus carota* antifreeze protein; DSC, differential scanning calorimetry; GSH, glutathione; SDTA, synchro different temperature analysis; TGA, thermal gravimetric analyses; THA, thermal hysteresis activity.

LITERATURE CITED

(1) Uhlig, S.; Wendel, A. The physiological consequences of glutathione variations. *Life Sci.* **1992**, *51*, 1083−1094.

(2) Rodriguez, J. V.; Mamprin, M. E.; Guibert, E. E.; Labadie, G. Protective effect of glutathione (GSH) over glutathione monoethyl-ester (GSH-E) on cold preservation of isolated rat liver cells. *Cell Transplant.* **1995**, *4*, 245−251.

(3) Vreugdenhil, P. K.; Belzer, F. O.; Southard, J. H. Effect of cold storage on tissue and cellular glutathione. *Cryobiology* **1991**, *28*, 143−149.

(4) Alvarez, J. G.; Storey, B. T. Spontaneous lipid peroxidation in rabbit epididymal spermatozoa: its effects on sperm motility. *Biol. Reprod.* **1982**, *27*, 1102−1108.

(5) Rodriguez, J. V.; Mamprin, M. E.; Mediavilla, M. G.; Guibert, E. E. Glutathione (GSH) movements during cold preservation of rat hepatocytes. *Cryobiology* **1998**, *36*, 236−244.

(6) Oyamada, T.; Fukui, Y. Oxygen tension and medium supplements for in vitro maturation of bovine oocytes cultured individually in a chemically defined medium. *J. Reprod. Dev.* **2004**, *50*, 107−117.

(7) Alvarez, J. G.; Storey, B. T. Evidence for increased lipid peroxidative damage and loss of superoxide dismutase activity as a mode of sublethal cryodamage to human sperm during cryopreservation. *J. Androl.* **1992**, *13*, 232−241.

(8) DeVries, A. L.; Wohlschlag, D. E. Freezing resistance in some Antarctic fishes. *Science* **1969**, *163*, 1073−1075.

(9) Yang, D. S. C.; Sicheri, F. Ice-binding structure and mechanism of an antifreeze protein from winter flounder. *Nature* **1995**, *375*, 427−431.

(10) Zhang, C.; Zhang, H.; Wang, L. Effect of carrot (*Daucus carota*) antifreeze protein on fermentation capacity of frozen dough. *Food Res. Int.* **2007**, *40*, 763−769.

(11) Yang, D. S. C.; Hon, W. C.; Bubanko, S.; Xue, Y.; Seetharaman, J.; Hew, C. L.; Sicheri, F. Identification of the ice-binding surface on a type III antifreeze protein with a "flatness" function algorithm. *Biophys. J.* **1998**, *74*, 2142−2151.

(12) Griffith, M.; Ewart, K. V. Antifreeze proteins and their potential use in frozen foods. *Biotechnol. Adv.* **1995**, *13*, 375−402.

(13) Payne, S. R.; Oliver, J. E.; Upreti, G. C. Effect of antifreeze proteins on the motility of ram spermatozoa. *Cryobiology* **1994**, *31*, 180−184.

(14) Younis, A. I.; Rooks, B.; Khan, S.; Gould, K. G. The effects of antifreeze peptide III (AFP) and insulin transferrin selenium (ITS) on cryopreservation of chimpanzee (*Pan troglodytes*) spermatozoa. *J. Androl.* **1998**, *19*, 207−214.

(15) Arav, A.; Carney, J. N.; Pease, G. R.; Liu, K. L. Recent developments in cryopreservation of stallion semen with special emphasis on thawing procedure using thermal hysteresis proteins. *Zygote* **1994**, *2*, 379−382.

(16) Prathalingam, N. S.; Holt, W. V.; Revell, S. G.; Mirczuk, S.; Fleck, R. A.; Watson, P. F. Impact of antifreeze proteins and antifreeze glycoproteins on bovine sperm during freeze-thaw. *Theriogenology* **2006**, *66*, 1894−1900.

(17) Tietze, F. Enzymic method for quantitative determination of nanogram amounts of total and oxidized glutathione. *Anal. Biochem.* **1969**, *27*, 502−522.

(18) Meyer, K.; Keil, M.; Naldrett, M. J. A leucine-rich repeat protein of carrot that exhibits antifreeze activity. *FEBS Lett.* **1999**, *447*, 171−178.

(19) Chen, T. C.; Zhang, J. Z.; Ye, W. Thermal hysteresis activity of antifreeze protein solution a direct differential scanning calorimetric measurment. *Acta Biophys. Sin.* **1996**, *12*, 39−42.

(20) Lucas, T.; Quellec, S.; LeBail, A.; Davenel, A. Chilling and freezing of part-baked bread. Part II: Experimental assessment of water phase changes and structure collapse. *J. Food Eng.* **2005**, *70*, 151−164.

(21) Riesen, R.; Vogel, K.; Schubnell, M. DSC by the TGA/SDTA851^e considering mass changes. *J. Therm. Anal. Calorim.* **2001**, *64*, 243−252.

(22) Soria, D. B.; Amalvy, J. I.; Piro, O. E.; Castellano, E. E.; Aymonino, P. J. Crystal and molecular structure determination, TGA, DTA and infrared and Raman spectra of rubidium nitroprusside monohydrate, $Rb_2[Fe(CN_5)NO]\cdot H_2O$. *J. Chem. Crystallogr.* **1999**, *26*, 325−330.

(23) Rikhvanov, E. G.; Varakina, N. N.; Rusaleva, T. M.; Rachenko, E. I.; Voinikov, V. K. The effect of sodium azide on the thermotolerance of the yeasts *Saccharomyces cerevisiae* and *Candida albicans*. *Microbiology* **2002**, *71*, 662−665.

(24) Zhou, X. L.; Chen, T. T.; Wang, B. H.; Li, Z. F.; Fei, Y. B.; Wei, L. B.; Gao, S. Q. DSC study on the thermal hysteresis activity of plant antifreeze protein. *Acta Phys. Chem. Sin.* **2001**, *17*, 66−69.

(25) Graham, L. A.; Liou, Y. C.; Walker, V. K.; Davies, P. L. Hyperactive antifreeze protein from beetles. *Nature* **1997**, *388*, 727−728.

(26) Deng, G.; Andrews, D. W.; Laursen, R. A. Amino acid sequence of a new type of antifreeze protein from the longhorn sculpin *Myoxocephalus octodecinspittosis*. *FEBS Lett.* **1997**, *402*, 17−20.

(27) Barrett, J. Thermal hysteresis proteins. *Int. J. Biochem. Cell Biol.* **2001**, *33*, 105−117.

(28) Jiang, Y.; Wei, L. B.; Fei, Y. B.; Shu, N. H.; Gao, S. Q. Purification and identification of antifreeze proteins in *Ammopiptanthus mongolicus*. *Acta Bot. Sin.* **1999**, *41*, 967−971.

(29) Hazen, K. C.; Hazen, B. W. Surface hydrophobic and hydrophilic protein alterations in *Candida albicans*. *FEMS Microbiol. Lett.* **1993**, *107*, 83−87.

(30) Gadea, J.; Selles, E.; Marco, M. A.; Coy, P.; Matas, C.; Romar, R.; Ruiz, S. Decrease in glutathione content in boar sperm after cryopreservation. Effect of the addition of reduced glutathione to the freezing and thawing extenders. *Theriogenology* **2004**, *62*, 690−701.

Received for review February 9, 2007. Revised manuscript received April 5, 2007. Accepted April 11, 2007.

JF070387Q